

Synthesis, *Spectrofluorometric* Studies, Micellization and non Linear Optical Properties of Blue Emitting Quinoline (AMQC) Dye

S. M. Afzal^{1,4} · Abdullah M. Asiri^{2,3} · M. A. N. Razvi¹ · Ahmed H. Bakry¹ · Salman A. Khan² · Mohie E. M. Zayed²

Received: 19 October 2015 / Accepted: 27 November 2015 / Published online: 18 January 2016
© Springer Science+Business Media New York 2016

Abstract Blue emitting 2-amino-4-(3, 4, 5-trimethoxyphenyl)-9-methoxy-5,6 dihydrobenzo[f]isoquinoline-1-carbonitrile (AMQC) dye was synthesized by one-pot multi-component reactions (MCRs) of 3,4,5-trimethoxybenzaldehyde, malononitrile, 6-methoxy-1,2,3,4-tetrahydro-naphthalin-1-one and ammonium acetate. Results obtained from spectroscopic and elemental analysis of synthesized AMQC was in good agreement with their chemical structures. Fluorescence polarity study demonstrated that AMQC was sensitive to the polarity of the microenvironment provided by different solvents. In addition, spectroscopic and physicochemical parameters, including electronic absorption, excitation coefficient, Stokes shift, oscillator strength, transition dipole moment and fluorescence quantum yield were investigated in order to explore the analytical potential of AMQC. Dye undergoes solubilization in different micelles and may be used as a quencher and a probe to determine the critical micelle concentration (CMC) of SDS and CTAB. Nonlinear optical parameters of AMQC dye shows relatively lower nonlinear refractive index and nonlinear absorption coefficient at the power levels. Variation of n_2 with concentration is linear in the concentration range used in the present study.

Keywords AMQC · Fluorescence quantum yield · CMC · Nonlinear refractive index

Introduction

In linear optics, various phenomena, like polarizability, absorption coefficient, refractive index, refraction etc., depend upon the wavelength of the incident light only but are independent of its intensity. In nonlinear optics [1] the interaction of radiation with matter depends upon the intensity of incident radiation also. After the advent of laser, several experiments have been carried out to demonstrate the nonlinear optical behavior of optical media. It was then established that the refractive index also depends upon intensity, violation of superposition principle has been, frequency of light can be altered when it passes through a nonlinear optical medium. In fact nonlinearity exists in the medium itself, rather than the incident radiation. Nonlinearity has given birth to several new applications, like second and third order harmonic generation, Kerr effect, nonlinear refraction, and absorption etc. New devices have been prepared on the basis of the nonlinear optical properties of some materials.

Recently third order effects and nonlinear refraction in organic dyes were studied. These dyes are having very high nonlinear refractive index and can be used as power limiting devices and also as optical switches [2–7]. These studies also lead to the compilation of several databases listing the nonlinear optical properties of various known crystals, liquids, gases, dyes [8].

Researchers have developed many techniques to measure the nonlinear refractive index and nonlinear absorption [9, 10] namely, phase distortion method [13] degenerate four wave mixing [11], nonlinear interferometry ellipse rotation [12]. Not only these techniques have very complicated

✉ Salman A. Khan
sahmad_phd@yahoo.co.in

¹ Physics Department, Faculty of Science, King Abdulaziz University, P.O. Box 80203, Jeddah 21589, Saudi Arabia

² Chemistry Department, Faculty of Science, King Abdulaziz University, P.O. Box 80203, Jeddah 21589, Saudi Arabia

³ The Center of Excellence for Advanced Materials, King Abdulaziz University, P.O. Box 80203, Jeddah 21589, Saudi Arabia

⁴ Physics Department, Aligarh Muslim University, Aligarh 202002, India

experimental setups but also very expensive instruments have been used. Recently Z-scan technique [14, 15] has been introduced which is very simple, low cost as well as highly sensitive. It is a single beam method, where principles of spatial beam distortion have been used to measure both the sign and magnitude of the optical nonlinearity. Due to its simplicity and easy determination of nonlinear absorption and nonlinear refraction in solids, liquids, composite glasses and semiconductor material [16, 17], now a days this technique has been used by several researchers.

Nitrogen containing organic molecules such as pyrazolines, pyrazoles, pyrimidines are important class of the heterocyclic compound in the field of medicinal chemistry. They are used as anti-bacterial [18], anti-tumor, anti-cancer [19], anti-viral agents [20]. During these days organic molecules are also applicable in the field of material sciences such as optical limiting [21], optical switching [22], electronic device [23], polymer coating [24], second order and third order non linear optical properties [25]. Due to numerous application of the nitrogen containing heterocyclic compounds, in this paper we prepared the new blue emitting 2-amino-4-(3, 4, 5-tri methoxyphenyl)-9-methoxy-5,6 dihydrobenzo[f]isoquinoline-1-carbonitrile (AMQC) dye and its physicochemical and non linear optical properties were investigated.

Experimental

Chemicals and Reagents

The 3,4,5-trimethoxybenzaldehyd, 6-methoxy-1,2,3,4-tetrahydro-naphthalin-1-one, malononitrile and ammonium acetate were purchased from Acros Organic. Other reagents and solvents (A.R.) were obtained commercially and used without further purification, except dimethylformamide (DMF), ethanol and methanol.

Apparatus

Melting points were recorded on a Thomas Hoover capillary melting apparatus without correction. FT-IR spectra were recorded on a Nicolet Magna 520 FT-IR spectrometer. $^1\text{H-NMR}$ and $^{13}\text{C-NMR}$ experiments were performed in CDCl_3 on a Bruker DPX 600 MHz spectrometer using tetramethyl silane (TMS) as internal standard at room temperature. UV-Vis electronic absorption spectra were acquired on a Shimadzu UV-1650 PC spectrophotometer. Absorption spectra were collected using a 1 cm quartz cell. Steady state fluorescence spectra were measured using Shimadzu RF 5301 PC spectrofluorophotometer with a rectangular quartz cell. Emission spectra were monitored at right angle. All fluorescence spectra were blank subtracted before proceeding in data analyses.

Z-Scan Measurement

The nonlinear refractive index n_2 and nonlinear absorption coefficient β have been measured by Z-scan technique, proposed by Shiek Bahae et al. [14], which is a very simple, yet highly sensitive technique, based on the principle of spatial beam distortion. This technique provides the value of nonlinear refractive index and its sign, and the nonlinear absorption coefficient. From these, the real and imaginary parts of the third order nonlinear susceptibility $\chi^{(3)}$ can easily be computed. An Ar ion laser Gaussian beam profile at 488 nm and power 75 mW is tightly focused by a convex lens having focal length of 50 mm. The sample is kept in 1 mm cuvette and is translated along the (Z-direction). The details of the experimental setup have been explained in our earlier papers [26, 27].

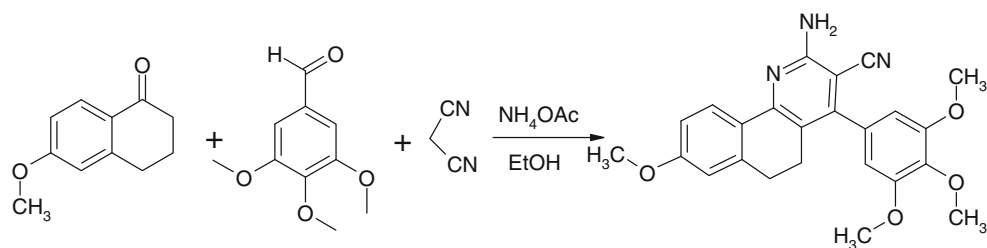
2-Amino-4-(3,4,5-tri Methoxyphenyl)-9-Methoxy-5,6 Dihydrobenzo[f]Isoquinoline-1-Carbonitrile (AMQC)

A one-pot mixture of the 3,4,5-trimethoxybenzaldehyd, (10 mmol), 6-methoxy-1,2,3,4-tetrahydro-naphthalin-1-one (1.46 g, 10 mmol), malononitrile (0.66 g, 10 mmol) and ammonium acetate (6.2 g, 80 mmol) in absolute ethanol (25 mL) was refluxed for 6 h [28]. The reaction mixture was allowed to cool, and the resulting precipitate was filtered, washed with water, dried and recrystallized from ethanol and chloroform. EI-MS m/z (rel. Int. %): 419 (62) $[\text{M} + 1]^+$; IR (KBr) ν_{max} cm^{-1} : 3452 (NH_2), 2954 (C-H), 2216 (CN), 1565 (C = C), 1258 (N = C); $^1\text{H NMR}$ (600MXz CDCl_3) δ : 8.14 (d, 1 H, CH_{Ar} , $J = 9.6$ Hz), 7.82 (s, 1 H, CH_{Ar}), 6.96 (d, 1 H, CH_{Ar} , $J = 2.4$ Hz), 6.92 (s, 1 H, CH_{Ar}), 6.68 (s, 1 H, CH_{Ar}), 5.16 (s, 2 H, NH_2), 3.98 (s, 3 H, OCH_3), 3.94 (s, 3 H, OCH_3), 3.86 (s, 3 H, OCH_3), 3.82 (s, 3 H, OCH_3), 2.78–2.74 (m, 2 H, C5), 2.68–2.56 (m, 2 H, C6); $^{13}\text{CNMR}$ (CDCl_3) δ : 162.56, 158.56, 157.58, 154.76, 152.72, 150.72, 149.16, 143.13, 141.86, 127.98 (Ar-C), 117.86 (CN), 115.72, 114.13, 113.12, 112.25, 108.36, 97.18, 95.24, 91.35, 56.70, 27.96 (C6), 26.12 (C5); Anal. calc. for $\text{C}_{24}\text{H}_{23}\text{N}_3\text{O}_4$: C, 69.05, H, 5.55, N, 10.07. Found: C, 68.88, H, 5.48, N, 9.82.

Result and Discussion

Chemistry

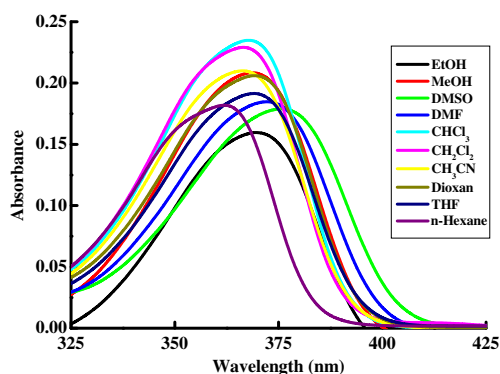
2-amino-4-(3, 4, 5-tri methoxyphenyl)-9-methoxy-5,6 dihydrobenzo [f] isoquinoline-1-carbonitrile (AMQC) was synthesized by one-pot multicomponent reactions (MCRs) of 3,4,5-trimethoxybenzaldehyd, malononitrile, 6-methoxy-1,2,3,4-tetrahydro-naphthalin-1-one and ammonium acetate (Scheme 1). The purified product was characterized by the FT-IR, $^1\text{H-NMR}$, $^{13}\text{C-NMR}$ and EI MS spectra. The IR spectrum of AMQC shows the characteristic band at 3452 cm^{-1}

Scheme 1 Synthesis of AMQC

due to presence -NH_2 group and at 2216 cm^{-1} attributed to the CN group. IR spectra shows sharp peak at 1258 cm^{-1} due presence of $\text{C}=\text{N}$ stretch which conforms to formation of quinoline. $^1\text{H-NMR}$ spectra, which prove diagnostic tool for the positional elucidation of the proton. Assignments of the signals are based on chemical shift and intensity pattern. The $^1\text{H-NMR}$ spectra of AMQC measured at room temperature shows one singlet at 5.16 ppm for the NH_2 . The appearance of three singlets at δ 7.82, 6.92 and 6.68 and two doublet at δ 8.14 and 6.96 was due to aromatic protons and two multiplets at δ 2.78–2.74 and 2.68–2.56 ppm corresponding to the benzylic protons ($\text{C}5\text{-H}$ and $\text{C}6\text{-H}$ respectively). Moreover, $^{13}\text{C-NMR}$ spectra showed signals at δ 27.96 ppm and at δ 26.12 ppm due to C6 and C5, respectively and the structure of the compounds was further confirmed due to presence of CN group at δ 117.86 ppm. Finally characteristic peaks were observed in the mass spectra of AMQC by the molecular ion peak. The mass spectrum of AMQC shows a molecular ion peak (M^+) m/z 419.

Spectral Behavior of 2-Amino-4-(3,4,5-tri Methoxyphenyl)-9-Methoxy-5,6 Dihydrobenzo[f] Isoquinoline-1-Carbonitrile (AMQC)

Absorption and emission spectra of $1 \times 10^{-5}\text{ mol dm}^{-3}$ AMQC dye in various non-polar, polar aprotic and protic solvents were studied (Fig 1 and Fig 2). Calculated physicochemical parameters obtained from steady state absorption and fluorescence spectra are tabulated in Table 1. As seen in Fig 1 polarity of solvent has an effect on the absorption maxima. AMQC show a broad absorption band at 368–384 nm region

**Fig. 1** Electronic absorption spectra of $1 \times 10^{-5}\text{ mol dm}^{-3}$ of AMQC in different solvents

with a red shift of 16 nm on going from n-hexane to DMSO indicating that the allowed transition is $\pi\text{-}\pi^*$ with charge transfer character. On excitation at 360 nm, the emission spectrum of AMQC shows a large red shift of 32 nm on changing the solvent polarity from n-hexane (400 nm) to DMSO (432 nm). This indicates that photoinduced intramolecular charge transfer (ICT) occurs in the singlet excited state from the electron donating substituent O-CH_3 group to the electron acceptor CN group of the molecule and therefore the polarity of AMQC increases on excitation. Further, a considerable difference in the magnitude of Stokes shift was observed from 2173 to 2893 cm^{-1} on changing the solvent polarity from non polar to polar, indicating that the excited state is different from the ground state. As seen in Fig. 1 and Fig. 2 absorption spectra show little sensitivity to change in solvent polarity, but emission spectra show a large red shift with increasing solvent polarity, confirming the presence of $\pi\text{-}\pi^*$ transitions in AMQC and stabilization of highly dipolar excited state in polar solvents.

The energy of absorption (E_a) and emission (E_f) spectra of the AMQC in different solvents correlated with the empirical Dimroth polarity parameter $E_T(30)$ [29] of the solvent (Fig. 3). A linear correlation between the energy of absorption and emission versus polarity of solvents was obtained (Eq. 1 and 2), implying potential application of these parameters to probe the microenvironment of AMQC.

$$E_a = 75.17 - 0.1032 \times E_T(30) \quad (1)$$

$$E_f = 68.28 - 0.257 \times E_T(30) \quad (2)$$

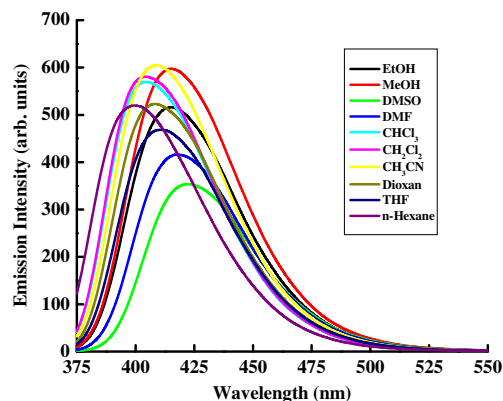
**Fig. 2** Emission spectra of $1 \times 10^{-5}\text{ mol dm}^{-3}$ of AMQC in different solvents

Table 1 Spectral data and fluorescence quantum yield (Φ_f) of AMQC dye in different solvents

Solvent	Δf	E_T^N	$E_T(30)$ Kcal mol ⁻¹	$\lambda_{ab}(nm)$	$\lambda_{em}(nm)$	ϵ M ⁻¹ cm ⁻¹	f	μ_{12} Debye	$\Delta\nu$ (cm ⁻¹)	Φ_f
EtOH	0.305	0.654	51.9	379	423	15,610	0.17	3.69	2745	0.43
MeOH	0.299	0.762	55.4	377	421	20,700	0.22	4.19	2773	0.38
DMSO	0.266	0.441	54.1	384	432	17,810	0.20	4.03	2893	0.26
DMF	0.263	0.404	43.8	380	426	18,490	0.21	4.11	2841	0.30
CHCl ₃	0.217	0.259	39.1	376	412	23,460	0.21	4.09	2324	0.23
CH ₂ Cl ₂	0.255	—	40.7	375	409	22,800	0.20	3.98	2217	0.32
Acetonitrile	0.304	0.472	45.6	373	417	20,840	0.23	4.26	2829	0.39
Dioxan	0.274	0.164	36	377	415	20,670	0.20	3.99	2429	0.33
THF	0.148	0.210	37.4	374	416	19,150	0.20	3.98	2699	0.29
n-Hexane	0.0014	—	31.1	368	400	18,300	0.15	3.41	2173	0.37

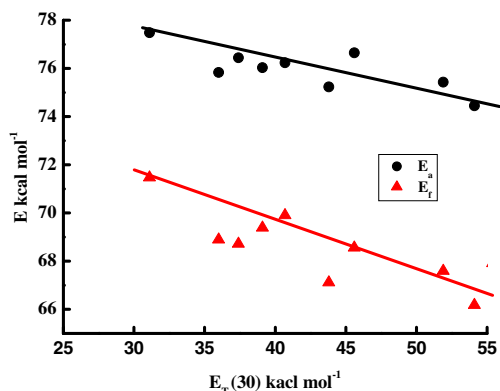
Determination of Oscillator Strength and Transition Dipole Moment

The solvatochromic performance of AMQC allows to establish the difference in the dipole moment between the excited singlet and the ground state ($\Delta\mu = \mu_e - \mu_g$). This variation can be obtained using the simplified Lippert- Mataga equation as follows [29, 30]:

$$\Delta\nu_{st} = \frac{2(\mu_e - \mu_g)^2}{hca^3} \Delta f + \text{Const.} \quad (3)$$

$$\Delta f = \frac{D-1}{2D+1} - \frac{n^2-1}{2n^2+1} \quad (4)$$

where $\Delta\nu_{st}$ is known as Stokes-shift which decreases with decrease in the solvent polarity indicating to weak stabilization of the excited state in non polar solvents [29]. Δf is the orientation polarizability of the solvent, μ_e and μ_g are the dipole moments in the excited and ground state, respectively which measures both electron mobility and dipole moment of the solvent molecule. c is the speed of light in vacuum, a is the Onsager cavity radius and h is Planck's constant, n and ϵ are the refractive index and dielectric

**Fig. 3** Plot of energy of absorption (E_a) and emission (E_f) versus $E_T(30)$ of different solvents

constant of the solvent in eq. 3 respectively. The Onsager cavity radius was chosen to be 4.2 Å because this value is comparable to the radius of a typical aromatic fluorophore [31].

$\Delta\nu_{ss}$ is the Stokes shifts of the AMQC in different solvents were deliberate, as shown in Table 1, using the following the equation [32]:

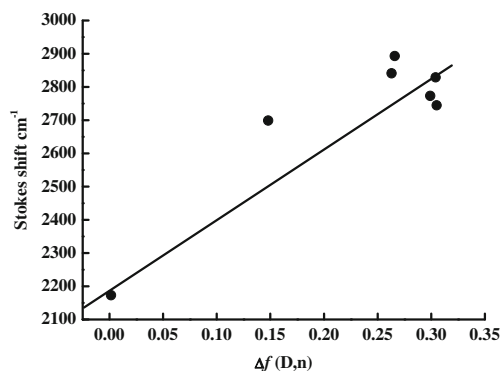
$$\Delta\nu_{ss} = \nu_{ab} - \nu_{em} \quad (5)$$

where $\Delta\nu_{ss}$ is the difference between λ_{max} of the ν_{ab} and ν_{em} indicate the wavenumbers of absorption and emission maxima (cm⁻¹) respectively.

The change in dipole moments ($\Delta\mu$) between the excited singlet and ground state were calculated from the slope of plot of Stokes shifts ($\Delta\nu_{ss}$) and orientation polarizability of the solvent (Δf) as 4.95 Debye for AMQC respectively Fig. 4, positive value indicating that the excited state is more polar than the ground state.

The change in transition dipole moments ($\Delta\mu_{12}$) between the excited singlet and ground state of AMQC in various solvents were calculated as in Table 1, using the eq. 6 [33].

$$\mu_{12}^2 = \frac{f}{4.72 \times 10^{-7} \times E_{max}} \quad (6)$$

**Fig. 4** Plot of Δf versus Stokes shift ($\Delta\nu$)

where E_{\max} is the maximum energy of absorption in cm^{-1} and f is the oscillator strength.

The oscillator strength (f), can be calculated using the following equation:

$$f = 4.32 \times 10^{-9} \int \varepsilon(\bar{\nu}) d\bar{\nu} \quad (7)$$

where $\bar{\nu}$ represents the numerical value of wavenumber (cm^{-1}) and ε is the extinction coefficient ($\text{Lmol}^{-1} \text{cm}^{-1}$). Oscillator strength values of AMQC in various solvents were calculated from the equation no. 7 and reported in Table 1, [34].

$E_T(30)$ and E_T^N is the empirical Dimroth polarity parameter of AMQC was also premeditated according to the following equation [35].

$$E_T^N = \frac{E_T(\text{solvent}) - 30.7}{32.4} \quad (8)$$

$$E_T(\text{solvent}) = \frac{28591}{\lambda_{\max}} \quad (9)$$

where λ_{\max} corresponds to the peak wavelength (nm) in the red region of the intramolecular charge transfer absorption of the bitain dye. AMQC has bathochromic when solvent polarity increase from n-hexane to DMSO indicates that the polarity of AMQC and photoinduced intramolecular charge transfer (ICT) occurs in the singlet excited state, therefore increasing the excitation.

Fluorescence Quantum Yield of AMQC

The fluorescence quantum yield (ϕ_f) was measured using the optically diluted solution to avoid reabsorption effect (absorbance at excitation wavelength); relative method with solution of 9, 10-diphenylanthralene (DPA) in DMSO as reference standard. The following relation has applied to calculate the fluorescence quantum yield [36]:

$$\phi_f(s) = \phi_f(r) \frac{F(s) \{1 - \exp(-A_{ref} \ln 10)\} \times n^2_s}{F(ref) \{1 - \exp(-A_s \ln 10)\} \times n^2_r} \quad (10)$$

where F denotes the integral of the corrected fluorescence spectrum, A is the absorbance at the excitation wavelength, and n is the refractive index of the medium. The subscripts “s” and “r” refer to sample and reference, respectively.

The fluorescence quantum yield (ϕ_f) of AMQC depends strongly on the solvent properties (Table 1). The fluorescence quantum yield can be correlated with $E_T(30)$ of the solvent, where $E_T(30)$ is the solvent polarity parameter introduced by Reichardt [37] Fig. 5. The fluorescence quantum yield (ϕ_f) of AMQC decreases with increasing solvent polarity. This could be attributed to efficient internal conversion and or

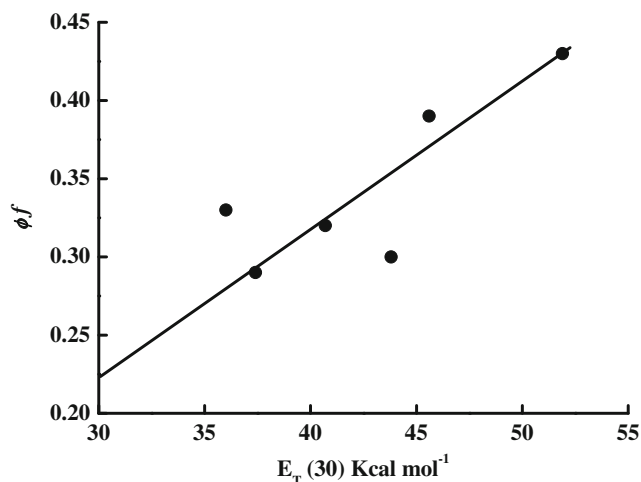


Fig. 5 Plot of ϕ_f versus $E_T(30)$ of different solvents

intersystem crossing by extensive mixing between the close-lying $^1(\pi-\pi^*)$ and $^1(n-\pi^*)$ states.

Effect of Surfactant on Emission Spectrum of AMQC

A positively charged and cetyltrimethyl ammonium bromide (CTAB) and negatively charged sodium dodecyl sulphate (SDS) surfactants were selected for evaluating the emission behavior of the AMQC dye. The two specified surfactants were chosen because ionic charges possessed by AMQC dye can be influenced by the positively charged CTAB and negatively charged SDS. Thus, the charge attraction accounts for the AMQC emission behavior. Fluorescence emission spectra of AMQC in the absence and presence of CTAB and SDS were measured. Fluorescence intensities of AMQC increase when increasing the concentration of CTAB from 2×10^{-4} up to 1.6×10^{-3} M as shown Fig. 6. Such enhancement in the fluorescence intensity of 1×10^{-5} M AMQC at fixed concentrations with an increase in the CTAB concentration may likely be ascribed to the association mechanism of AMQC with CTAB. The fluorescence intensity of AMQC is quenched with an increase of the SDS concentration (2×10^{-3} up to 1.6×10^{-2} M). Moreover, more significant reductions were

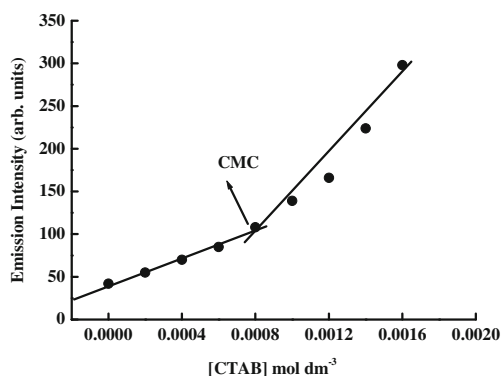


Fig. 6 Plot of I_f versus concentration of CTAB for AMQC dye

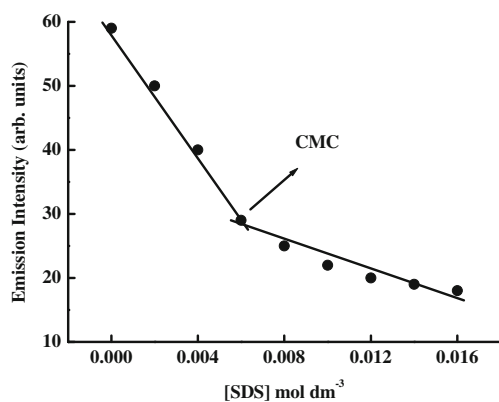


Fig. 7 Plot of I_f versus concentration of SDS for AMQC dye

noticed in fluorescence intensities of AMQC with SDS. The quenching of AMQC upon increasing SDS concentration can likely be ascribed to the association of AMQC with SDS. Figure 7 represents the influence of SDS on the relative emission intensity of 1×10^{-5} M AMQC. It can be observed that there was a subsequent decrease in the relative emission intensity of AMQC with an increase in the SDS concentration, strongly providing that there was an interaction between AMQC and SDS. It seems that the dye molecule located in the hydrocarbon core of CTAB aggregates, while in SDS, the dye located at micelle – water interface, with quenching role of water. As shown in Fig 6 & Fig 7, the emission intensity of AMQC increases with increasing the concentration of surfactant CTAB, and emission intensity of AMQC decreases with increasing the concentration of surfactant SDS an abrupt change in fluorescence intensity is observed at surfactant concentration of 7.96×10^{-4} and 6.10×10^{-3} mol dm⁻³ which are very close to the critical micelle concentration of CTAB and SDS [38] respectively; thus AMQC can be employed as a probe to determine the CMC of a surfactants Fig. 6 and Fig. 7. It was well known that aromatic molecules were generally solubilized in the palisade layer of micelle [39]. Thus the enhancement of emission intensity is attributed to the

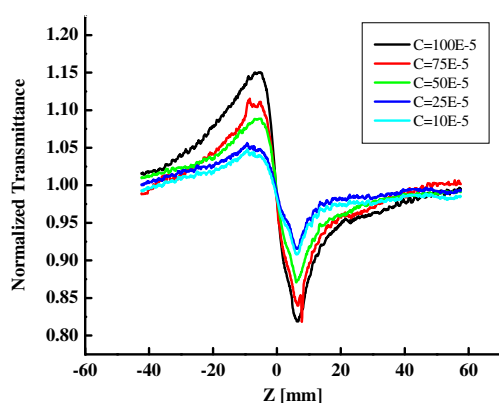


Fig. 8 Close aperture scan at concentrations 1 mM, 0.75 mM, 0.5 mM, 0.25 mM and 0.1 mM of AMQC dye

Table 2 Nonlinear refractive index and $\chi^{(3)}$ of blue emitting dye at $\lambda = 488$ nm and Power = 75 mW of AMQC dye

Concentration (mM)	$n_2 \times 10^{-9}$ (cm ² /W)	$\chi^{(3)} \times 10^{-7}$ (esu)
1	-14.92	7.88
0.75	-10.54	5.56
0.5	-9.05	4.79
0.25	-5.50	2.91
0.1	-1.88	1.09

passage of dye molecule from the aqueous bulk solution to the palisade layer of micelle.

Nonlinear Measurements

Z-scan measurements were carried out to measure the sign and magnitude of nonlinear refractive index and nonlinear absorption. The intensity dependent nonlinear absorption and refraction are related by the following equations [15, 40]

$$\alpha(I) = \alpha_0 + \beta I \quad (11)$$

$$n(I) = n_0 + n_2 I \quad (12)$$

where α_0 is the linear absorption coefficient, n_0 is the linear refractive index, β and n_2 are the nonlinear absorption coefficient and refractive index respectively. I is the intensity of the input laser beam.

Closed aperture Z-scan measurements were carried out to measure the nonlinear refractive index of AMQC. Figure 8 shows the variation of normalized transmittance versus Z-position for the different concentrations from 1 mM to 0.1 mM of the dye dissolved in chloroform $CHCl_3$. The plot shows a pre focal transmittance maximum (peak) followed by a post focal transmittance minimum (valley) which is the signature of negative nonlinear refractive index.

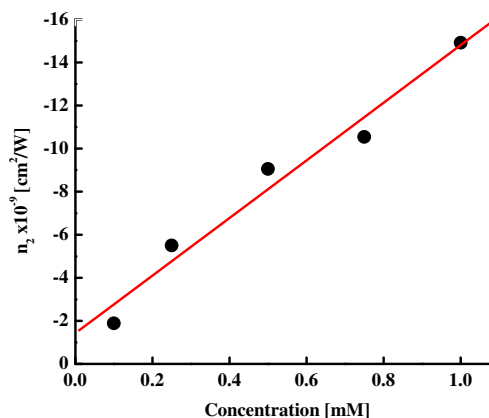


Fig. 9 Variation of nonlinear refractive index n_2 with concentration of AMQC dye

We have evaluated the nonlinear refractive index, n_2 and the nonlinear absorption coefficient β by fitting the normalized transmittance of close aperture scan data with the following equation [41]

$$T(\text{close}) = 1 + \frac{2(-\rho x^2 + 2x - 3\rho)}{(x^2 + 9)(x^2 + 1)} \Delta\Phi_0 \quad (13)$$

where, $\rho = \frac{\Delta\psi}{\Delta\Phi_0}$; $\Delta\Phi_0 = kn_2 L_{\text{eff}} I_0$ and $\Delta\psi = \beta I_0 \frac{L_{\text{eff}}}{2}$ are the phase shifts due to nonlinear refraction and nonlinear absorption. $x = \frac{z}{z_0}$ is related to diffraction length of the beam, $z_0 = \frac{kw_0^2}{2}$; $L_{\text{eff}} = \frac{[1 - \exp(-\alpha_0 L)]}{\alpha_0}$, which is effective thickness of the sample, α_0 is linear absorption coefficient, L is the actual thickness of the sample, I_0 is the on-axis irradiance at the focus $I_0 = \frac{2P}{\pi w_0^2}$. w_0 is the beam waist at focus. The values for the nonlinear refractive index, n_2 at different concentration are summarized in Table 2. However the values of β obtained by the least square fit of above equation are very low and inconsistent. In order to evaluate nonlinear absorption, we also recorded the open aperture Z-scan data. The scan reveals a flat horizontal line for the normalized transmittance. This indicates the value of nonlinear absorption is very low for this dye. So it is not possible for us to measure β from this data. Hence it confirms the results obtained from closed aperture scan data. We also calculated the values of $x^{(3)}$ based on the standard equations [14, 17], taking $\beta=0$, and these are also presented in Table 2.

As it is an established fact that the nonlinear refraction arises from thermal, electrostrictive, molecular and electronic effects. But in our case origin of the nonlinearity is mainly due to thermal effects since we have used a cw laser [42]; it is also evident from peak-valley separation being more than 1.7 times the Rayleigh range z_0 . Figure 9 shows the variation of nonlinear refractive index versus concentrations. It is observed that as the concentration increases the (negative) nonlinearity also increases.

Conclusion

Blue emitting dye 2-amino-4-(3, 4, 5-tri methoxyphenyl)-9-methoxy-5,6 dihydrobenzo [f] isoquinoline-1-carbonitrile (AMQC) was synthesized by one-pot multicomponent reactions (MCRs). AMQC dye displays red shift in fluorescence spectrum as solvent polarity increases. AMQC dye undergoes solubilization in different micelles and may be used in the determination of CMC of surfactants (e.g. SDS and CTAB) and it can be used as quencher or probe for dyes. Nonlinear optical parameters of AMQC dye shows relatively lower nonlinear refractive index and nonlinear absorption coefficient at

the power levels. Variation of n_2 with concentration is linear in the concentration range used in the present study. Although the dye has excellent fluorescence yield in the blue spectral region, however it has relatively poor nonlinear response at the operating parameters.

Acknowledgments This Project was funded by Saudi Basic Industries Corporation (SABIC) and the Deanship of Scientific Research (DSR), King Abdulaziz University, Jeddah, under grant no. 25-130-1436-S. The authors, therefore, acknowledge with thanks SABIC and DSR technical and financial support.

References

- Boyd RW (2008) *Nonlinear Optics*, 3rd edn. Academic Press, Boston Rochester, New York
- Shettigar S, Umesh G, Purnesh P, Manjunatha KB, Asiri AM (2009) The third-order nonlinear optical properties of novel styryl dyes. *Dyes Pigments* 83:207–210
- Sun R, Yan B, Ge J, Xu Q, Li N, Wu X, Song Y, Lu J (2013) Third-order nonlinear optical properties of unsymmetric pentamethine cyanine dyes possessing benzoxazolyl and benzothiazolyl groups. *Dyes Pigments* 96:189–195
- Al-Ahmad AY, Hassan QMA, Badran HA, Hussain KA (2012) Investigating some linear and nonlinear optical properties of the azo dye (1-amino-2-hydroxy naphthalin sulfonic acid-[3-(4-azo)]-4-amino diphenyl sulfone). *Opt Laser Technol* 44:1450–1455
- He T, Wang C, Zhang C, Lu G (2011) Nonlinear optical properties of an azo-based dye irradiated by picosecond and nanosecond laser pulses. *Phys B Condens Matter* 406:488–493
- Li D, Yu D, Zhang Q, Li S, Zhou H, Wu J, Tian Y (2013) Synthesis, crystal structure and third-order nonlinear optical properties in the near-IR range of a novel stilbazolium dye substituted with flexible polyether chains. *Dyes Pigments* 97:278–285
- Castanon SL, Beristain MF, Ortega A, Gomez-Sosa G, Munoz E, Perez-Martinez AL, Ogawa T, Halim MF, Smith F, Walser A, Dorsinville R (2011) The synthesis, characterization and third-order nonlinear optical character of poly(2,5-dipropargyloxybenzoate) containing a polar aromatic diacetylene. *Dyes Pigments* 88:129–134
- Marvin J, Weber editor-in-chief (2002) *Handbook of Optical Materials*. CRC Press, Boca Raton
- Weber MJ, Milam D, Smith WL (1978) Nonlinear refractive index of glasses and crystals. *Opt Eng* 17:463–465
- Moran MJ, She CY, Carman RL (1975) Interferometric Measurement of the Nonlinear Refractive -Index coefficient Relative to CS₂ in Laser system-Related materials. *IEEE J Quantum Electron QE-11:259–263*
- Friberg SR, Smith PW (1987) Nonlinear refractive index of glasses for ultrafast optical switches. *IEEE J Quantum Electron QE-23:2089–2094*
- Owyoung A (1973) Ellipse Rotation studies in Host Materials. *IEEE J Quantum Electron QE-9:1064–1069*
- Williams WE, Soileau MJ, Van Stryland EW (1984) Optical switching and n_2 measurements in CS₂. *Opt Commun* 50:256–263
- Sheik-Bahae M, Said AA, Van Stryland EW (1989) High-sensitivity, single-beam n_2 measurements. *Opt Lett* 14:955–957
- Sheik-Bahae M, Said AA, Wei T, Hagan DJ, Van Stryland EW (1990) IEEE sensitive measurements of optical nonlinearities using a single beam. *J Quantum Electron QE-26:760–769*
- Wang J, Sheik-Bahae M, Said AA, Hagan DJ, Van Stryland EW (1994) Time-resolved Z-scan measurements of optical nonlinearities. *J Opt Soc Am B* 11:1009–1017

17. Said AA, Sheik-Bahae M, Hagan DJ, Wei TH, Wang J, Young J, Ven Stryland EW (1992) Determination of bound and free carrier nonlinearities in ZnSe, GaAs, CdTe and ZnTe. *J Opt Soc Am B* 9: 405–414
18. Asiri AMSA, Khan SA (2012) Synthesis, characterization, and in vitro antibacterial activities of macromolecules derived from bis-chalcone Abdullah M. Asiri, Salman a. Khan. *J Heterocycl Chem* 49:1434–1438
19. Mamtimin X, Matsidik R, Nurulla I (2010) New soluble rigid rod copolymers comprising alternating 2-amino-pyrimidine and phenylene repeat units: syntheses, characterization, optical and electrochemical properties. *Polymer* 51:437–446
20. Koytepe S, Paşahan A, Ekinci E, Seçkin T (2005) Synthesis, characterization and H₂O₂-sensing properties of pyrimidine-based hyperbranched polyimides. *Eur Polym J* 41:121–127
21. Zhang Q, Luo J, Ye L, Wang H, Huang B, Zhang J, Wu J, Zhang S, Tian Y (2014) Design, synthesis, linear and nonlinear photophysical properties and biological imaging application of a novel Λ -type pyrimidine-based thiophene derivative. *J Mol Struct* 1074:33–42
22. Achelle S, Ramondenc Y, Dupas G, Ple N (2008) Bis- and tris(arylethynyl)pyrimidine oligomers: synthesis and light-emitting properties. *Tetrahedron* 12:2783–2791
23. Baranov VI, Gribov LA, Djenjer VO, Zelentsov DY (1997) Adiabatic semi-empirical parametric method for computing electronic-vibrational spectra of complex molecules part 3. *Azines. J Mol Struct* 407:209–216
24. Jacobs JF, Koper GJM, Ursem WJ (2007) UV protective coatings: a botanical approach. *Prog Org Coat* 58:166–171
25. Asiri AM, Khan SA (2011) Synthesis, characterization and optical properties of mono- and bis-chalcone. *Mater Lett* 65:1749–1752
26. Razvi MAN, Bakry AH, Afzal SM, Khan SA, Abdullah M, Asiri AM (2015) Synthesis, characterization and determination of third-order optical nonlinearity by cw z-scan technique of novel thiobarbituric acid derivative dyes. *Mater Lett* 144:13
27. Khan SA, Razvi MAN, Bakry AH, Afzal SM, Asiri AM, El-Daly SA (2015) Microwave assisted synthesis, spectroscopic studies and non linear optical properties of bis-chromophores. *Spectrochim Acta A* 137:1100
28. Asiri AM, Khan SA, Al-Thaqafy SH, Sharma K (2015) One pot synthesis, photophysical and X-ray studies of novel highly fluorescent isoquinoline derivatives with higher antibacterial efficacy based on the in-vitro and density functional theory. *J Fluoresc* 2015:503–518
29. Chakraborty A, Kar S, Nath DN, Guchhait N (2007) Photoinduced intramolecular charge-transfer reactions in 4-amino-3-methyl benzoic acid methyl ester: A fluorescence study in condensed phase and jet-cooled molecular beams. *J Chem Sci (Indan Academy of Science)* 119:195–203
30. Asiri AM, Khan SA, Marwani HM, Sharma K (2013) Synthesis, spectroscopic and physicochemical investigation of environmentally benign heterocyclic Schiff base derivatives as antibacterial agents on the bases of in vitro and density functional theory. *J Photochem Photobiol B*: 120:82–89
31. Suppan S. (1990) Invited review solvatochromic shifts: the influence of the medium on the energy of electronic states. *J. Photochem. Photobiol., A*: 50: 293–330.
32. Bordeau G, Lartia R, Teulade-Fichou M (2010) Meta-substituted triphenylamines as new dyes displaying exceptionally large Stokes shifts. *Tetrahedron Lett* 51:4429
33. Aktan E, Babür B, Seferoğlu Z, Hokelek T, Şahin E (2011) Synthesis and structure of a novel heterozyloindole dye studied by X-ray diffraction, FT-IR, FT-Raman, UV-vis, NMR spectra and DFT calculations. *J Mol Struct* 1002:113–120
34. Kawashita Y, Yabana K, Noda M, Nobusada K, Nakatsukasa T (2009) Oscillator strength distribution of C₆₀ in the time-dependent density functional theory. *J Mol Struct* 914:130–135
35. El-Daly S, Asiri AM, Khan SA, Alamry KA (2013) Ravi Spectral Properties and Micellization of 1-(2, 5-Dimethyl-thiophen-3-yl)-3-(2, 4, 5-trimethoxy-phenyl)-propenone (DTTP) in Different Media. *J Lumin* 134:819–824
36. Kotaka H, Konishi G, Mizuno K (2010) Synthesis and photoluminescence properties of π -extended fluorene derivatives: the first example of a fluorescent solvatochromic nitro-group-containing dye with a high fluorescence quantum yield. *Tetrahedron Lett* 51:181–184
37. Royzen M, Canary JW (2013) Structural parameters of Zn(II) complexes of 8-hydroxyquinoline-based tripodal ligands affect fluorescence quantum yield. *Polyhedron* 58:85–91
38. Mukherjee K, Moulik SP, Mukherjee DC (1993) Thermodynamics of micellization of aerosol OT in polar and nonpolar solvents. *A Calorimetric Study Langmuir* 9:1727–1730
39. Mukerjee P, Cardinal JR (1978) Benzene derivatives and naphthalene solubilized in micelles. Polarity of microenvironments, location and distribution in micelles, and correlation with surface activity in hydrocarbon-water systems. *J Phys Chem* 82:1620–1627
40. Sutherland RL (1966) *Handbook of Nonlinear Optics*. Marcel Dekker, Inc, New York
41. Liu X, Guo S, Wang H, Hou L (2001) Theoretical study on the closed aperture z-scan curves in the materials with nonlinear refraction and strong nonlinear absorption. *Opt Commun* 197:431–438
42. Christodoulides DN, Khoo IC, Salamo GJ, Stegeman GI, Van Stryland EW (2010) Nonlinear refraction and absorption: mechanisms and magnitudes. *Adv Opt Photon* 2:60